Study on Creep Parameters and Long-Term Strength of White Sandstone under the Coupling Effect of Chemical Corrosion and Temperature

Yong Wang*, Qin Xu, Ye Zhou, Jiahong Wang, Mo Xiao, Guifei Wang

School of Science, Qingdao University of Technology, Qingdao, 266520, SD, PR China

*Correspondence: wang_yong@qut.edu.cn

Abstract

To quantitatively analyze the influence of coupled chemical corrosion and temperature effects on the creep characteristic parameters of white sandstone, the instantaneous strain, steady-state creep rate, and long-term strength were extracted based on uniaxial stepwise loading creep tests. The results indicate that under acidic or alkaline environments, the instantaneous strain and steady-state creep rate at each loading level gradually increase with rising temperature, exhibiting minor variations within the range of 0–50 °C but showing a significant increase after 75 °C. Under neutral environments, both parameters increase slowly. At the same temperature, the instantaneous strain and steady-state creep rate rank in the order of acidic > alkaline > neutral conditions. The long-term strength is approximately 70 % of the instantaneous strength and decreases with increasing temperature, with a more pronounced decline after 75 °C; the lowest long-term strength is observed under acidic conditions. Temperature primarily affects the creep parameters by accelerating the rate of chemical reactions, and the deterioration of creep parameters induced by chemical corrosion and temperature effects exhibits a mutually reinforcing and superimposed promoting effect. This study provides a basis for the environmental impact assessment of rock creep parameters.

Keywords

White sandstone; instantaneous strain; steady-state creep rate; long-term strength; temperature–chemical coupling.

1. INTRODUCTION

The creep behavior of rocks is typically quantified using parameters including instantaneous strain, steady-state creep rate, and long-term strength. These parameters serve as critical bases for stability analysis of surrounding rock and support design in underground engineering. In practical engineering scenarios, surrounding rock is often subjected to the combined effects of chemical corrosion by groundwater and geothermal temperature variations. Thus, investigating the variation laws of creep parameters of white sandstone under the coupled action of chemical corrosion and temperature holds important practical engineering significance.

At present, scholars at home and abroad have carried out certain studies on the effects of single factors (i.e., chemical corrosion or temperature) on rock creep parameters. In terms of chemical corrosion, Wang Yongyan et al. [1,2] established creep equations for sandstone under chemical corrosion; Wang Yanchun et al. [3,4] analyzed the influence of pH on the instantaneous strain and steady-state creep rate of shale. Regarding temperature effects, Qin Nan et al. [5] investigated the variations of creep parameters of soft rock under temperature-pressure coupling; Zhou Guanglei et al. [6] developed a time-dependent creep model for rock under temperature-stress coupling. In the aspect of chemical-temperature coupling, Wang Yanchun [7] conducted creep tests on shale under temperature-chemical coupling, but the study mainly focused on the morphological analysis of creep curves, with less quantitative research on creep parameters.

Recent studies have addressed various aspects of rock and material mechanics [8–15], including water-bearing soft rock creep, deep tunnel deformation, layered rock creep modeling, backfill and tailings management, FRP composites, slag in UHPC, and CO_2-activated cementitious materials. However, the evolution of rock creep parameters under coupled chemical–thermal conditions (below 100 °C) remains poorly understood.

To address this gap, this study investigates white sandstone sampled from Zigong, Sichuan Province. After coupled conditioning with various chemical solutions (H_2SO_4 at pH = 1, distilled water, and NaOH at pH = 13) at different temperatures (0 °C, 25 °C, 50 °C, 75 °C, and 100 °C), uniaxial stepwise loading creep tests were carried out. The instantaneous strain and steady-state creep rate corresponding to each loading level were determined, and isochronal stress–strain curves were constructed to evaluate the long-term strength. The evolutionary characteristics of creep parameters under diverse coupled conditions were systematically examined, and the coupled deterioration mechanism of chemical corrosion and temperature on the creep parameters of white sandstone was ultimately elucidated.

2. ROCK SAMPLE PREPARATION AND TESTING SCHEME

Table 1. Temperature and chemical solution settings

Specimen group	Immersion solution	pH value	Solution concentration (mol/L)	Solution volume (L)	Temperature (°C)
A0	H2SO4	1	0.1	20	0
A25	H2SO4	1	0.1	20	25
A50	H2SO4	1	0.1	20	50
A75	H2SO4	1	0.1	20	75
A100	H2SO4	1	0.1	20	100
B0	Distilled water	7	0	20	0
B25	Distilled water	7	0	20	25
B50	Distilled water	7	0	20	50
B75	Distilled water	7	0	20	75
B100	Distilled water	7	0	20	100
C0	NaOH	13	0.1	20	0
C25	NaOH	13	0.1	20	25
C50	NaOH	13	0.1	20	50
C75	NaOH	13	0.1	20	75
C100	NaOH	13	0.1	20	100

ISSN: 2472-3703 DOI: 10.6911/WSRJ.202608_12(8).0003

White sandstone from Zigong, Sichuan, was machined into Φ50 mm × 100 mm cylindrical specimens, with end non-parallelism < 0.05 mm and axial deviation < 0.25°. After drying at 25 °C for 96 h, specimens were immersed in H_2SO_4 (pH = 1), distilled water (pH = 7), and NaOH (pH = 13), and heated to 0, 25, 50, 75, and 100 °C. pH was monitored and adjusted daily until stable at 100 °C, when specimens were removed.

The uniaxial creep test was conducted using a stepwise loading method on a TAW-200 testing machine. The initial load was set to 8 kN (4 MPa), with each subsequent loading increment of 8 kN (4 MPa) at a loading rate of 50 N/s. Each load level was maintained for 4 h, and the stepwise loading was continued until specimen failure occurred. The specific grouping of the coupled chemical corrosion and temperature treatment is presented in Table 1.

3. TEST RESULTS AND ANALYSIS

3.1. Characteristics of Instantaneous Strain Variation

To facilitate a more precise comparison of the instantaneous strain of white sandstone under different coupled chemical corrosion and temperature conditions, the creep curves of the white sandstone were compiled and summarized in Table 2.

Table 2. Instantaneous strain at different stress levels (×10^{-3})

pH value	Temperature (°C)	Stress (MPa)					
		4	8	12	16	20	24
1	0℃	3.8	5.8	7.1	8.5	10.0	11.8
	25℃	3.9	5.9	7.2	8.6	9.9	11.9
	50℃	4.0	6.0	7.4	8.7	10.1	12.0
	75℃	5.1	7.7	9.5	11.1	13.0	—
	100℃	7.1	9.9	12.0	14.5	—	—
7	0℃	3.3	5.0	6.1	7.3	8.4	9.9
	25℃	3.2	5.1	6.2	7.2	8.5	10.0
	50℃	3.3	5.1	6.3	7.4	8.6	10.1
	75℃	3.5	5.4	6.6	7.8	9.0	10.4
	100℃	3.8	5.7	6.9	8.1	9.1	10.7
13	0℃	3.6	5.5	6.8	8.1	9.4	10.9
	25℃	3.7	5.6	6.9	8.1	9.3	10.9
	50℃	3.8	5.6	6.8	8.0	9.4	11.0
	75℃	4.7	7.0	8.5	10.0	11.9	—
	100℃	6.4	9.0	11.0	13.2	—	—

Table 2 presents the instantaneous strain of white sandstone subjected to different coupled chemical corrosion and temperature conditions. As can be observed from the table, for each specimen under any given coupled condition, the instantaneous strain at each subsequent loading level consistently exceeds that at the preceding level. Notably, the increments of instantaneous strain at the first and final loading levels (the latter corresponding to the accelerated creep stage) are more pronounced than those at the intermediate levels.

This phenomenon can be attributed to the following mechanisms. Upon application of the first load, the pre-existing microcracks within the sandstone close under compression, giving rise to relatively large deformation and thus a greater strain increment. At the intermediate loading levels, although new microcracks continue to form, the degree of closure of pre-existing cracks is substantially reduced compared with that at the first loading stage, resulting in relatively smaller strain increments. At the final loading stage (accelerated creep), internal

ISSN: 2472-3703 DOI: 10.6911/WSRJ.202608_12(8).0003

microcracks proliferate and small fissures progressively coalesce into larger macrocracks, leading to an increase in both crack quantity and size. Consequently, the deformation resistance of the sandstone deteriorates, and the corresponding strain increment again becomes relatively large.

Under the same chemical environment (acidic or alkaline), the instantaneous strain at each loading level increases gradually with rising temperature (below 100 °C). At 0 °C, 25 °C, and 50 °C, the strain values remain relatively close and exhibit little variation; however, a substantial increase is observed beyond 75 °C. In neutral environment, the instantaneous strain at each loading level rises only slightly with increasing temperature and remains generally stable.

At a given temperature, the instantaneous strain at each loading level in both acidic and alkaline environments is greater than that in neutral environment. Furthermore, a distinct difference exists between acidic and alkaline conditions, with the strain under acidic immersion being consistently larger than that under alkaline immersion.

The underlying mechanisms can be summarized as follows. In acidic or alkaline environments, chemical reactions take place between the mineral constituents of the sandstone and the reactive ions (H^+ or OH^-) in the solutions, resulting in the formation of new pores, the enlargement of pre-existing ones, and occasionally the healing of certain defects. Elevated temperatures, particularly above 75 °C, accelerate the kinetics of these reactions. The reactivity of the sandstone components with H^+ ions in acidic solution is greater than that with OH^- ions in alkaline solution. In neutral environment, temperature elevation below 100 °C does not induce significant structural alteration of the rock matrix; thus, thermal damage remains minor and can be considered negligible. Temperature primarily contributes to rock degradation by accelerating the chemical reaction rates, thereby reducing the overall strength of the material.

3.2. Characteristics of Steady-State Creep Rate Variation

Table 3. Steady-state creep rate of white sandstone at different stress levels ($\times 10^{-3}$)

pH value	Temperature (°C)	Stress (MPa)					
		4	8	12	16	20	24
1	0°C	0.07	0.11	0.16	0.22	0.28	0.36
	25°C	0.07	0.12	0.17	0.22	0.28	0.37
	50°C	0.08	0.13	0.18	0.22	0.29	0.38
	75°C	0.11	0.17	0.24	0.32	0.43	—
	100°C	0.16	0.25	0.35	0.50	—	—
7	0°C	0.04	0.06	0.08	0.11	0.15	0.22
	25°C	0.05	0.07	0.10	0.14	0.18	0.25
	50°C	0.05	0.07	0.11	0.15	0.19	0.26
	75°C	0.06	0.08	0.11	0.15	0.21	0.29
	100°C	0.07	0.10	0.14	0.19	0.25	0.34
13	0°C	0.06	0.10	0.14	0.19	0.25	0.33
	25°C	0.07	0.11	0.15	0.20	0.26	0.34
	50°C	0.07	0.12	0.16	0.21	0.26	0.35
	75°C	0.10	0.16	0.23	0.30	0.40	—
	100°C	0.14	0.23	0.33	0.46	—	—

ISSN: 2472-3703 DOI: 10.6911/WSRJ.202608_12(8).0003

Through a preliminary analysis of the creep curves of white sandstone, the general characteristics of its creep behavior were obtained. As is well known, the steady-state creep rate is one of the most important parameters in the study of rock creep properties. It refers to the constant strain rate maintained during the steady-state creep stage. The steady-state creep rate holds significant reference value in both the safety evaluation of rock engineering and the development of creep models. Based on the obtained creep test data and the plotted creep curves, the steady-state creep rate of white sandstone was calculated. The steady-state creep rates of white sandstone under different coupled chemical corrosion and temperature conditions are presented in Table 3.

Table 3 summarizes the steady-state creep rates of white sandstone measured at various stress levels. It is evident from the data that, under the same temperature condition, the steady-state creep rate at each loading step is higher in acidic and alkaline solutions than in neutral solution. In addition, the creep rates differ between the acidic and alkaline cases, with the acidic immersion yielding consistently larger values than the alkaline one.

These differences are mainly due to chemical interactions between the sandstone minerals and the ions in the solutions. In acidic and alkaline media, H^+ and OH^- ions react with the mineral phases, which may either create new defects or heal existing ones. The reaction with H^+ ions appears to be more intensive than that with OH^- ions.

To provide a clearer comparison of the steady-state creep rate under different coupled chemical and thermal conditions, the data from Table 3 were further processed and plotted using Origin software. The resulting curves, illustrating the variation of steady-state creep rate with axial load, are presented in Fig. 1.

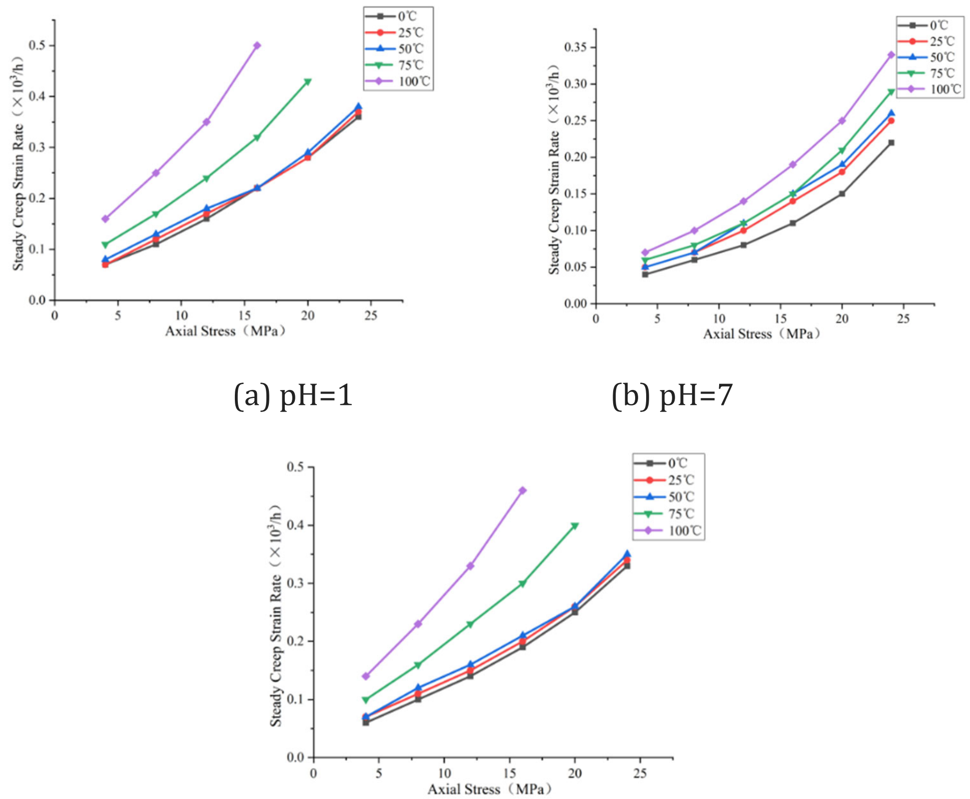

(a) pH=1 (b) pH=7

(c) pH=13

Figure 1. Variation of steady-state creep rate with axial load at different temperatures

ISSN: 2472-3703 DOI: 10.6911/WSRJ.202608_12(8).0003

Fig. 1 illustrates the variation of steady-state creep rate with axial load at different temperatures. In conjunction with the data presented in Table 3, the following trends can be discerned from the figure. Under acidic, neutral, and alkaline conditions, the steady-state creep rate at each loading level increases progressively with increasing axial load. Moreover, the increment in the steady-state creep rate from one loading level to the next is consistently greater than the preceding increment.

This behavior can be explained by the progressive development of internal damage within the specimens. As the axial load increases, new microcracks initiate and small fissures gradually propagate into larger cracks, resulting in an increase in both crack number and crack size. Consequently, the deformation resistance of the white sandstone deteriorates, leading to a continuously increasing increment in the steady-state creep rate with each successive loading step.

Furthermore, based on the data compiled in Table 3, the relationship between the steady-state creep rate and temperature was established and is presented in Fig. 2.

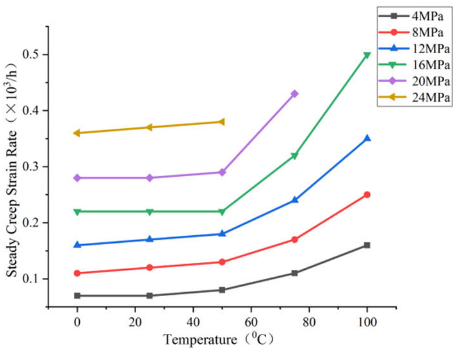

(a) pH=1

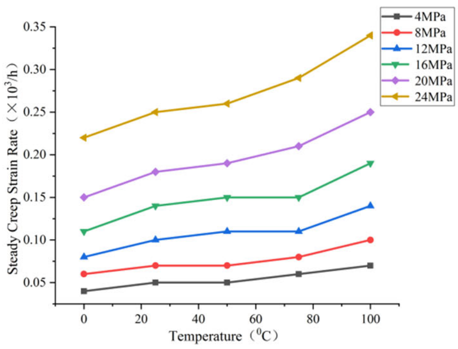

(b)pH=7

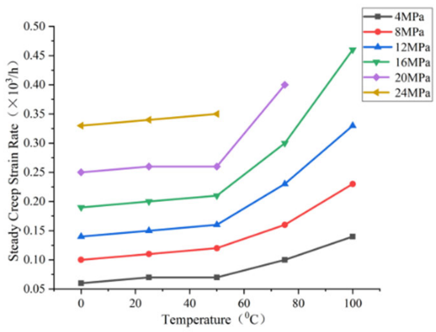

(c) pH=13

Figure 2. Variation of steady-state creep rate with temperature under different loading conditions

Fig. 2 illustrates the variation of steady-state creep rate with temperature under different loading conditions. In conjunction with the data listed in Table 2, several trends can be observed. In acidic or alkaline environments, the steady-state creep rate at each loading level exhibits a gradual upward trend with increasing temperature (below 100 °C). At 0 °C, 25 °C, and 50 °C, the creep rates remain relatively close to one another, showing little variation; however, a marked increase occurs once the temperature exceeds 75 °C. Under neutral conditions, by contrast, the steady-state creep rate at each loading level rises only marginally with temperature and remains essentially stable throughout the tested temperature range.

ISSN: 2472-3703 DOI: 10.6911/WSRJ.202608_12(8).0003

These observations can be attributed to the following mechanisms. Acidic and alkaline solutions induce internal deterioration of the sandstone structure, manifesting as the formation or sealing of defects, the creation of new pores, and the enlargement of existing ones. Such chemical attacks are substantially accelerated at elevated temperatures, particularly above 75 °C. In neutral environments, however, temperature variations below 100 °C do not produce any appreciable alteration in the rock framework; consequently, thermal damage is minimal and can be considered negligible. Overall, temperature exerts its influence primarily by accelerating the rates of chemical reactions, thereby promoting microstructural degradation and reducing the macroscopic strength of the rock.

3.3. Isochronal Stress–Strain Curves and Long-Term Strength Analysis

Following the acquisition of creep curves from the test data of white sandstone, equally spaced time points were selected along the abscissa (time axis) of each curve to obtain the corresponding strain values at different stress levels for each identical time instant. In this way, a series of stress–strain curves at specific creep durations were constructed, which are designated as isochronal stress–strain curves. By applying this procedure, the isochronal stress–strain curves of white sandstone specimens immersed in solutions of varying pH values at 25 °C were plotted, as presented in Fig. 3.

It should be noted that during the creep tests, the loading process of the testing machine is not instantaneous but requires a finite period of time to complete, thereby occupying a portion of the overall test duration. Consequently, in the construction of the isochronal stress–strain curves, the point at time zero was not adopted. Instead, the point corresponding to 0.05 h, i.e., the moment when the designated load level was fully applied, was taken as the initial reference. As a result, the isochronal stress–strain curves presented herein do not commence from the origin of the coordinate axes.

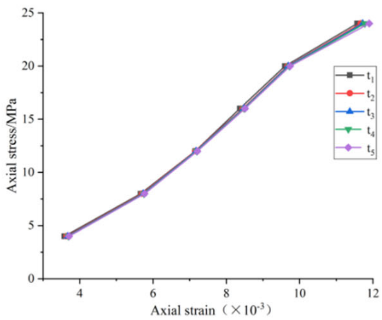

(a) pH=1

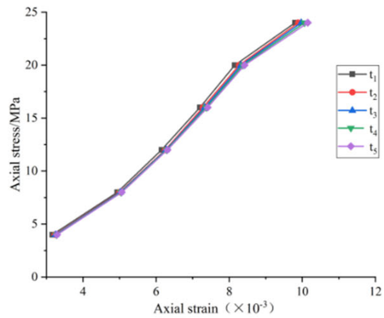

(b) pH=7

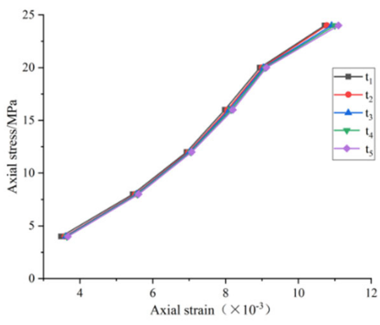

(c) pH=13

Figure 3. Isochronal stress–strain curves at 25 °C

ISSN: 2472-3703 DOI: 10.6911/WSRJ.202608_12(8).0003

Fig. 3 presents the isochronal stress–strain curves of white sandstone at 25 °C, where t_1, t_2, t_3, t_4, and t_5 denote the curves corresponding to creep deformation and stress at 0.05 h, 0.5 h, 1 h, 1.5 h, and 2.5 h, respectively. From the figure, the following observations can be made.

At 25 °C, the isochronal stress–strain curves of white sandstone immersed in solutions with different pH values essentially consist of three segments separated by two inflection points, namely a linear segment followed by two nonlinear segments. Upon transition from the linear segment to the first nonlinear segment, the slope increases and continues to rise progressively throughout the first nonlinear segment. Upon transition from the first nonlinear segment to the second nonlinear segment, the slope decreases and continues to decline progressively throughout the second nonlinear segment.

At 25 °C, the isochronal stress–strain curves for different pH solutions nearly overlap. Moreover, the isochronal stress–strain curve corresponding to a longer creep time (e.g., t_5) lies below that corresponding to a shorter creep time (e.g., t_1).

Rocks may exhibit either stable or unstable creep, depending primarily on the magnitude of the applied stress. When the stress exceeds a certain critical value, the creep tends to develop into unstable creep; when the stress remains below this critical value, the creep tends to develop into stable creep. This critical stress is commonly referred to as the long-term strength of the rock. In other words, long-term strength is defined as the strength value at which a rock resists failure under prolonged loading. Since rocks undergo creep effects under long-term loading, the creep strength is taken as the long-term strength.

Currently, two methods are commonly employed to determine the long-term strength of rocks: the transitional creep method and the isochronal curve method. The transitional creep method defines the maximum load at which the steady-state creep rate is zero as the long-term strength. Although this method is relatively straightforward, it is difficult in practice to directly identify the stress level corresponding to a zero steady-state creep rate, and the process is time-consuming and labor-intensive. The isochronal curve method determines the long-term strength as the stress value corresponding to the asymptote formed when the straight portions of the isochronal curves transition into curves. The inflection point of each isochronal curve marks the transition of the rock from the viscoelastic stage to the viscoplastic stage, indicating that the internal structure of the rock begins to change and damage initiates. The advantages of the isochronal curve method include the requirement of fewer specimens and higher efficiency. Therefore, this study adopts the isochronal curve method to determine the long-term strength of white sandstone under different coupled chemical corrosion and temperature conditions.

According to the principle of the isochronal curve method, an inflection point (the junction between the first and second nonlinear segments) can be identified on the isochronal stress–strain curves in Fig. 3(a). This inflection point represents the critical point at which the white sandstone transitions from the viscoelastic stage to the viscoplastic stage, and the corresponding stress value is taken as the long-term strength. Accordingly, the long-term strength of white sandstone immersed in acidic solution at 25 °C is determined to be 19.5 MPa. By applying the same procedure, the long-term strengths of white sandstone under other coupled chemical corrosion and temperature conditions were obtained, as listed in Table 4.

Table 4 presents the long-term strength of white sandstone under different coupled chemical corrosion and temperature conditions. From the table, the following observations can be made.

The long-term strength of white sandstone varies considerably across different coupled conditions; nevertheless, under each condition, it remains approximately 70 % of the corresponding instantaneous strength.

ISSN: 2472-3703 DOI: 10.6911/WSRJ.202608_12(8).0003

Table 4. Long-term strength of rock specimens under different conditions

Specimen label	Immersion solution	pH value	Temperature (°C)	Instantaneous strength (MPa)	Long-term strength (MPa)
A0	H2SO4	1	0	27.5	19.8
A25	H2SO4	1	25	26.5	19.5
A50	H2SO4	1	50	26.0	18.7
A75	H2SO4	1	75	21.0	14.8
A100	H2SO4	1	100	13.5	9.4
B0	Distilled water	7	0	30.5	21.6
B25	Distilled water	7	25	30.1	21.5
B50	Distilled water	7	50	29.9	21.2
B75	Distilled water	7	75	29.2	20.5
B100	Distilled water	7	100	27.1	19.8
C0	NaOH	13	0	28.8	20.7
C25	NaOH	13	25	28.6	20.4
C50	NaOH	13	50	28.5	20.4
C75	NaOH	13	75	25.0	17.1
C100	NaOH	13	100	18.7	13.0

Under identical chemical conditions (whether acidic or alkaline), the long-term strength tends to decrease gradually with rising temperature (below 100 °C). At 0 °C, 25 °C, and 50 °C, the long-term strength values remain fairly close to one another, showing little variation; however, a marked reduction occurs once the temperature exceeds 75 °C. Under neutral conditions, by contrast, the long-term strength decreases only marginally with increasing temperature and remains essentially stable throughout the tested temperature range.

At a given temperature, the long-term strength in acidic and alkaline environments is lower than that in neutral environment. Furthermore, the long-term strength differs between acidic and alkaline conditions, with acidic immersion yielding consistently lower values than alkaline immersion.

The underlying mechanisms can be summarized as follows. In acidic or alkaline environments, chemical reactions take place between the mineral constituents of the sandstone and the ions (H^+ or OH^-) present in the solutions. These reactions may lead to the formation of new pores, the enlargement of existing ones, and the creation or sealing of defects. Elevated temperatures, particularly above 75 °C, accelerate the rates of these chemical reactions. The degree of reaction between the sandstone components and H^+ ions is more pronounced than that with OH^- ions. In neutral environments, temperature variations below 100 °C do not cause any appreciable change in the rock fabric; consequently, thermal damage is minimal and may be regarded as negligible. Overall, temperature exerts its influence primarily by accelerating the rates of chemical reactions, thereby promoting microstructural deterioration and reducing the long-term strength of the rock.

ISSN: 2472-3703 DOI: 10.6911/WSRJ.202608_12(8).0003

4. CONCLUSIONS

Based on the experimental results and analysis presented above, the following main conclusions can be drawn:

(1) Under identical chemical conditions (acidic or alkaline), the instantaneous strain and steady-state creep rate at each loading level increase progressively with rising temperature. Variations remain minor within the range of 0 °C to 50 °C, but a marked increase is observed beyond 75 °C. Under neutral conditions, both parameters show only a slight increase with temperature and remain essentially stable.

(2) At a given temperature, the instantaneous strain and steady-state creep rate follow the order: acidic environment > alkaline environment > neutral environment. The highest values of both parameters are recorded under acidic immersion, followed by alkaline immersion, with the lowest values under neutral immersion.

(3) At 25 °C, the isochronal stress–strain curves of white sandstone immersed in solutions with different pH values consist of a linear segment followed by two nonlinear segments. The curves under different pH conditions nearly coincide, and the curve corresponding to a longer creep time lies below that corresponding to a shorter creep time.

(4) Under various coupled conditions, the long-term strength of white sandstone is approximately 70 % of its instantaneous strength. In acidic or alkaline environments, the long-term strength decreases gradually with increasing temperature, with little variation observed between 0 °C and 50 °C, but a pronounced reduction occurs beyond 75 °C. Under neutral conditions, the long-term strength decreases only slightly. At the same temperature, the long-term strength follows the order: neutral > alkaline > acidic.

(5) Temperature below 100 °C exerts a limited direct effect on the creep parameters; it primarily aggravates rock deterioration by accelerating chemical reaction rates. The influences of chemical corrosion and temperature on the creep parameters are mutually reinforcing and collectively promote the degradation of the rock.

Funding: This work was supported by the Qingdao Natural Science Foundation (24-4-4-zrjj-80-jch).

Data Availability Statement: The data used to support the findings of this study are available from the corresponding author upon request.

Conflicts of Interest: The authors declare that there are no conflicts of interest regarding the publication of this article.

REFERENCES

[1] Wang, Y. Y., Lü, Y. M., & Xiao, Z. J. (2010). Study on creep model of sandstone under chemical corrosion. Journal of China Coal Society, 35(7), 1095–1098. (in Chinese)

[2] Lü, Y. M. (2010). Study on the influence of chemical corrosion on creep characteristics of deep soft rock [Doctoral dissertation]. Qingdao University of Science and Technology. (in Chinese)

[3] Wang, Y. C., Wang, Y. Y., & Li, J. G. (2019). Creep model of shale based on chemical pH characterization. Journal of China Coal Society, 44(S2), 117–124. https://doi.org/10.13225/j.cnki.jccs.2019.0468 (in Chinese)

[4] Wang, Y. C., Wang, Y. Y., & Li, J. G. (2019). Study on creep mechanism of shale under chemical corrosion effect. Safety in Coal Mines, 50(8), 67–71. (in Chinese)

[5] Qin, N. (2014). Study on the influence of pressure and temperature on strength, damage energy dissipation and creep of soft rock-like materials [Doctoral dissertation]. Qingdao University of Science and Technology. (in Chinese)

ISSN: 2472-3703 DOI: 10.6911/WSRJ.202608_12(8).0003

[6] Zhou, G. L., Xu, T., Zhu, W. C., Chen, C. F., & Yang, T. H. (2017). A time-dependent creep model for rock under temperature–stress coupling. Engineering Mechanics, 34(10), 1–9, 25. https://doi.org/10.6052/j.issn.1000-4750.2016.05.0376 (in Chinese)

[7] Wang, Y. C. (2013). Study on creep behavior of deep soft rock under temperature–stress–chemical coupled fields [Doctoral dissertation]. Qingdao University of Science and Technology. (in Chinese)

[8] Zheng, Z. Q., Zhuo, L., & Pei, J. L. (2026). Creep of water-bearing soft rock and its influence on long-term rock mass stability. Engineering Geology, 362, 108505. https://doi.org/10.1016/j.enggeo.2026.108505

[9] Jing, W., Zhou, J., Yuan, L., & Wang, S. (2024). Deformation and failure mechanism of surrounding rock in deep soft rock tunnels considering rock rheology and different strength criteria. Rock Mechanics and Rock Engineering, 57(1), 545–580. https://doi.org/10.1007/s00603-023-03564-7

[10] Song, T. X., Feng, X. T., Zhou, Y. Y., Yang, C. X., & Yu, X. J. (2024). Anisotropic characteristics and creep model for thin-layered rock under true triaxial compression. Journal of Rock Mechanics and Geotechnical Engineering, 16(12), 4815–4834. https://doi.org/10.1016/j.jrmge.2024.01.006

[11] Behera, S. K., Mishra, D. P., Singh, P., & Mishra, A. K. (2021). Utilization of mill tailings, fly ash and slag as mine paste backfill material: Review and future perspective. Construction and Building Materials, 309, 125120. https://doi.org/10.1016/j.conbuildmat.2021.125120

[12] Qi, C. C., & Fourie, A. (2019). Cemented paste backfill for mineral tailings management: Review and future perspectives. Minerals Engineering, 144, 106025. https://doi.org/10.1016/j.mineng.2019.106025

[13] Harle, S. M. (2024). Durability and long-term performance of fiber reinforced polymer (FRP) composites: A review. Structures, 60, 105881. https://doi.org/10.1016/j.istruc.2024.105881

[14] Heraiz, H., Li, J. J., Pan, Z. P., Zhang, Y., & Wang, H. (2025). The utilization of slag, steel slag, and desulfurization gypsum as binder systems in UHPC with iron tailings and steel fibers—A review. Minerals, 15(5), 538. https://doi.org/10.3390/min15050538

[15] Cui, K., Zhao, D. Y., Zhao, Y. L., & Poon, C. S. (2026). Development of CO_2-induced SCMs for calcium sulfoaluminate cement: Towards enhancing hydration, compressive strength and later stage-ettringite stability. Cement and Concrete Research, 201, 108121. https://doi.org/10.1016/j.cemconres.2026.108121